JOURNAL OF GUIDANCE, CONTROL, AND DYNAMICS
Vol. 32, No. 3, May–June 2009

Engineering Notes

ENGINEERING NOTES are short manuscripts describing new developments or important results of a preliminary nature. These Notes should not exceed 2500 words (where a figure or table counts as 200 words). Following informal review by the Editors, they may be published within a few months of the date of receipt. Style requirements are the same as for regular contributions (see inside back cover).

Escape from Elliptic Orbit Using Constant Radial Thrust

Giovanni Mengali* and Alessandro A. Quarta†
University of Pisa, 56122 Pisa, Italy

DOI: 10.2514/1.43382

Introduction

THE classical problem of escape from a circular orbit using a constant radial thrust was first proposed by Tsien [1] and then refined by Battin [2]. The same problem was then revisited by Prussing and Coversone [3], providing more analytical results and introducing the concept of a potential-energy well. The aim of this Note is to show that the available results for circular orbits can be extended to elliptic orbits. In particular, two main issues are presented: 1) analytical expressions (in terms of propulsive acceleration) for the occurrence of an escape condition and 2) simple formulas for the maximum amplitude of the radial oscillation if escape does not occur. Although the following discussion is general, a mission with a constant radial thrust may be interpreted as a special case of minimagnetospheric plasma propulsion [4] (M2P2) in which the M2P2 system uses a nuclear power source [5].

Problem Formulation

Consider a spacecraft moving in an elliptic parking orbit around a primary body with gravitational parameter μ. Let a_0 and e_0 be the orbit semimajor axis and eccentricity, respectively. The spacecraft is equipped with a propulsion system capable of providing a constant radial outward propelling acceleration:

$$f_r = \eta\mu/a_0^2 \tag{1}$$

where η is a dimensionless parameter. Assume that the propulsion system is switched on at the time $t_0 \triangleq 0$, when the spacecraft true anomaly is $\nu_0 \triangleq \nu(t_0)$, and that it remains on for the whole mission length.

The spacecraft radial distance r from the primary body is described by the following second-order differential equation [2,3]:

$$\ddot{r} = \frac{a_0\mu(1-e_0^2)}{r^3} - \frac{\mu}{r^2} + \eta\frac{\mu}{a_0^2} \tag{2}$$

Multiplying both sides of Eq. (2) by $\dot{r}$ and integrating with respect to time between t_0 and $t > t_0$ yields [2]

$$\frac{\dot{r}^2}{2} = -\frac{a_0\mu(1-e_0^2)}{2r^2} + \frac{\mu}{r} + \eta\frac{\mu}{a_0^2}(r-r_0) + \mathcal{E}_0 \tag{3}$$

where

$$r_0 \triangleq r(t_0) = a_0(1-e_0^2)/(1+e_0\cos\nu_0)$$

is the initial spacecraft-primary distance and

$$\mathcal{E}_0 \triangleq -\mu/(2a_0) < 0$$

is the specific mechanical energy of the parking orbit. Because the specific mechanical energy of the osculating orbit for $t \geq t_0$ is, by definition,

$$\mathcal{E} = \frac{\dot{r}^2}{2} + \frac{a_0\mu(1-e_0^2)}{2r^2} - \frac{\mu}{r} \tag{4}$$

from Eq. (3), one has

$$\mathcal{E} = \mathcal{E}_0 + \eta\frac{\mu}{a_0^2}(r-r_0) \tag{5}$$

which quantifies the effect of the propulsion system on the osculating orbit energy as a function of the spacecraft distance from the primary body.

According to Battin [2], Eq. (3) provides a constraint on the mechanical energy that must be met by the spacecraft at all time instants. In fact, because $\dot{r}^2 \geq 0$, from Eq. (4), one has

$$\mathcal{E} \geq \frac{a_0\mu(1-e_0^2)}{2r^2} - \frac{\mu}{r} \tag{6}$$

Define

$$\mathcal{B} = \frac{1+e_0\cos\nu_0}{2} \tag{7}$$

and introduce the dimensionless radial distance $\tilde{r} \triangleq r/r_0$ and the dimensionless specific total energy $\tilde{\mathcal{E}} \triangleq \mathcal{E}/(\mu/r_0)$. Equations (5) and (6) can be rearranged in a more convenient form as

$$\tilde{\mathcal{E}} = \tilde{\mathcal{E}}_0 + 4\tilde{\mathcal{E}}_0^2\eta(\tilde{r}-1) \tag{8}$$

$$\tilde{\mathcal{E}} \geq \tilde{\mathcal{E}}_{\mathcal{B}} \tag{9}$$

where

$$\tilde{\mathcal{E}}_0 \triangleq \frac{\mathcal{E}_0}{\mu/r_0} = \frac{e_0^2-1}{4\mathcal{B}} \tag{10}$$

$$\tilde{\mathcal{E}}_{\mathcal{B}} \triangleq \frac{\mathcal{B}}{\tilde{r}^2} - \frac{1}{\tilde{r}} \tag{11}$$

The spacecraft motion, subject to a pure radial constant thrust, is therefore described by Eqs. (8) and (9). The effect of different initial spacecraft positions (in terms of true anomaly ν_0) can be taken into account by varying the value of $\mathcal{B}$. Equations (8) and (9) can be

Received 22 January 2009; revision received 9 February 2009; accepted for publication 13 February 2009.

*Associate Professor, Department of Aerospace Engineering, g.mengali@ing.unipi.it. Member AIAA.
†Research Assistant, Department of Aerospace Engineering, a.quarta@ing.unipi.it. Senior Member AIAA.

translated in a graphical form in the $\tilde{r}$–$\tilde{\mathcal{E}}$ plane. In fact, Eq. (8) describes a family of lines, passing through the point $P_1 = (1, \tilde{\mathcal{E}}_0)$, for which the angular coefficient depends on η: that is, on the propulsion system characteristics. Equation (9), taken with the equality sign, describes a family of curves, all passing through the point $P_2 = (1, \mathcal{B} - 1)$, and for which the shape is independent of η. The graphical arrangement corresponding to an orbital eccentricity $e_0 = 0.3$ and an initial true anomaly $\nu_0 = 60$ deg ($\tilde{\mathcal{E}}_0 = -0.396$ and $\mathcal{B} = 0.575$) is shown in Fig. 1.

It may be checked that points P_1 and P_2 coincide when circular parking orbits are considered ($e_0 = 0$). They also coincide for elliptic orbits ($e_0 < 1$), provided that the spacecraft is either at the pericenter ($\nu_0 = 0$) or at the apocenter ($\nu_0 = \pi$). In all of the other cases [that is, if $e_0 \in (0, 1)$ and $\nu_0 \neq (0, \pi)$], the ordinate of P_1 is always greater than that of P_2.

The gray zone below the curve $\tilde{\mathcal{E}}_{\mathcal{B}}(\tilde{r})$ (solid line in Fig. 1) characterizes a body region in which the spacecraft motion is unfeasible, as it would violate the constraint $\tilde{\mathcal{E}} \geq \tilde{\mathcal{E}}_{\mathcal{B}}$ of Eq. (9).

Return now to the straight line $\tilde{\mathcal{E}} = \tilde{\mathcal{E}}(\tilde{r})$ (dashed line in Fig. 1) described by Eq. (8). When $\eta = 0$, the line is horizontal (that is, the energy is constant), as implied by a perfectly Keplerian motion. Also, with reference to points in the half-plane $\tilde{r} \geq 1$, the line $\tilde{\mathcal{E}}(\tilde{r})$ intersects the curve $\tilde{\mathcal{E}}_{\mathcal{B}}(\tilde{r})$ in P_0 (see Fig. 1). As η is increased, the line slope increases as well, and as long as $0 < \eta < \eta^\star$, there are two intersections of the line with $\tilde{\mathcal{E}}_{\mathcal{B}}(\tilde{r})$. The critical value $\eta^\star$ is obtained when $\tilde{\mathcal{E}}(\tilde{r})$ is tangent (in the point $P^\star$) to $\tilde{\mathcal{E}}_{\mathcal{B}}(\tilde{r})$. In the figure example, the tangent condition is obtained when $\eta = \eta^\star \simeq 0.1011$. Finally, when $\eta > \eta^\star$, no intersections with $\tilde{r} > 1$ occur. This graphical representation allows one to locate a circle, centered at the attractor's center of mass, within which the spacecraft motion is confined to take place. In fact, for a given value of η, the spacecraft mechanical energy varies with $\tilde{r}$ according to Eq. (8), and therefore the spacecraft maximum achievable distance from the attractor body corresponds to the smaller abscissa (greater than 1) of the intersection points between $\tilde{\mathcal{E}}(\tilde{r})$ and $\tilde{\mathcal{E}}_{\mathcal{B}}(\tilde{r})$. The situation is better understood by investigating the spacecraft motion using the same initial conditions of the previous example ($e_0 = 0.3$ and $\nu_0 = 60$ deg) and a thrust level slightly less or greater than the critical value $\eta^\star$. In particular, Fig. 2 shows the trajectory and the time evolution of orbital eccentricity and semimajor axis for $\eta = 0.999\eta^\star$. The simulation length is $15T_0$, where $T_0 = 2\pi\sqrt{a_0^3/\mu}$ is the period of the parking orbit. As expected, the orbital elements have a periodic variation [2], but an escape does not occur. A substantially different result is obtained with a thrust level $\eta = 1.001\eta^\star$. Figure 3 shows that, in this case, an escape does occur at about $t/T_0 = 5.62$.

In summary, the condition $0 \leq \eta \leq \eta^\star$ characterizes a region (hatched in Fig. 1) in which the spacecraft motion is trapped around the primary. This region is the natural extension to an elliptic orbit problem of the concept of a potential well introduced in [3]. Note that

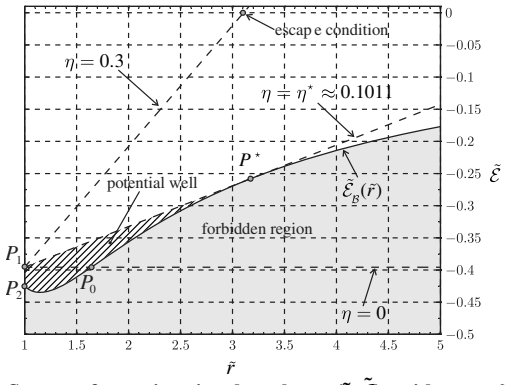

Fig. 1 Spacecraft motion in the plane $(\tilde{r}, \tilde{\mathcal{E}})$ with $e_0 = 0.3$ and $\nu_0 = 60$ deg; dashed lines correspond to Eq. (8), and the solid line refers to Eq. (11).

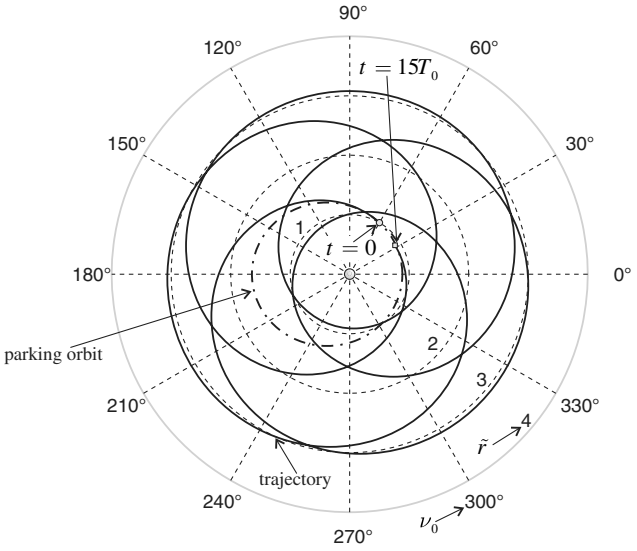

a) Spacecraft trajectory

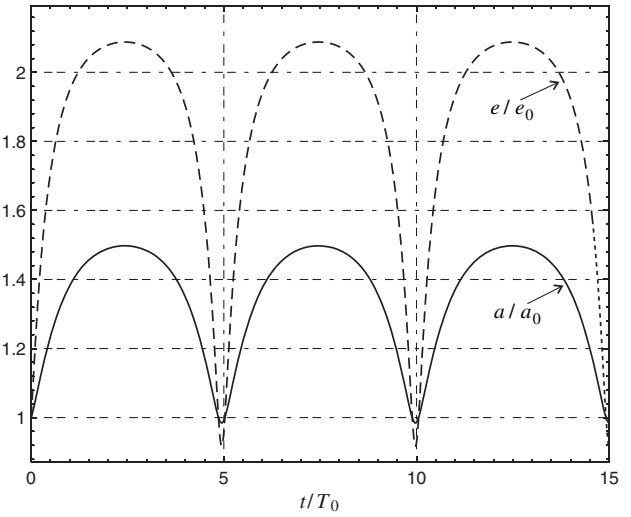

b) Time evolution of orbital parameters

Fig. 2 Spacecraft motion with $e_0 = 0.3$, $\nu_0 = 60$ deg, and $\eta = 0.999\eta^\star$.

$\eta = \eta^\star$ represents the least admissible thrust value that allows a spacecraft to go indefinitely away from the attractor and to eventually reach an escape condition (mathematically characterized by $\tilde{\mathcal{E}} = 0$).

From an analytical point of view, the region of admissible motion is characterized through the roots of the third-order polynomial $\mathcal{P}$ obtained by enforcing the equality $\tilde{\mathcal{E}} = \tilde{\mathcal{E}}_{\mathcal{B}}$ [that is, by equating the right members of Eqs. (8) and (11)]:

$$\mathcal{P} = 4\tilde{\mathcal{E}}_0^2\eta\tilde{r}^3 + (\tilde{\mathcal{E}}_0 - 4\tilde{\mathcal{E}}_0^2\eta)\tilde{r}^2 + \tilde{r} - \mathcal{B} \tag{12}$$

Recall from our previous discussion that in the range of $0 < \eta < \eta^\star$ there exist three real roots of $\mathcal{P}$, referred to as $\alpha < \beta < \gamma$. The first two ($\alpha \leq 1$ and $\beta \geq 1$) correspond, respectively, to the minimum and maximum achievable distances from the primary body, whereas γ is not physically reachable by the spacecraft because it is outside the potential well. When $\eta > \eta^\star$, $\mathcal{P}$ admits a unique real root $\alpha \leq 1$ because the spacecraft is now capable of storing an amount of energy sufficient to reach an escape condition. Finally, in absence of thrust ($\eta = 0$), $\mathcal{P}$ reduces to a second-order polynomial that can be factorized as

$$\mathcal{P}(\eta = 0) = \tilde{\mathcal{E}}_0(\tilde{r} - \tilde{r}_A)(\tilde{r} - \tilde{r}_P) \tag{13}$$

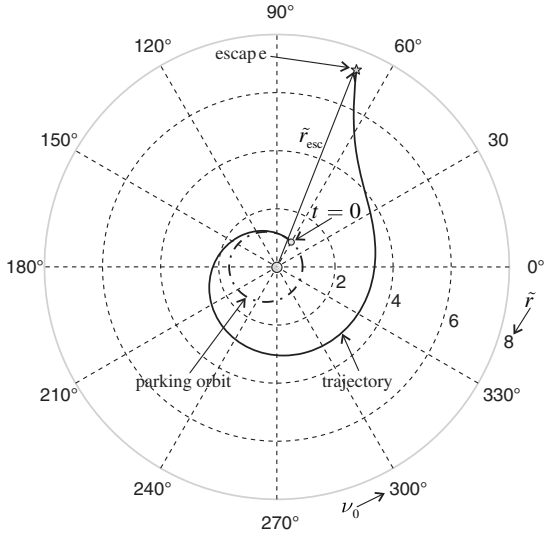

a) Spacecraft trajectory

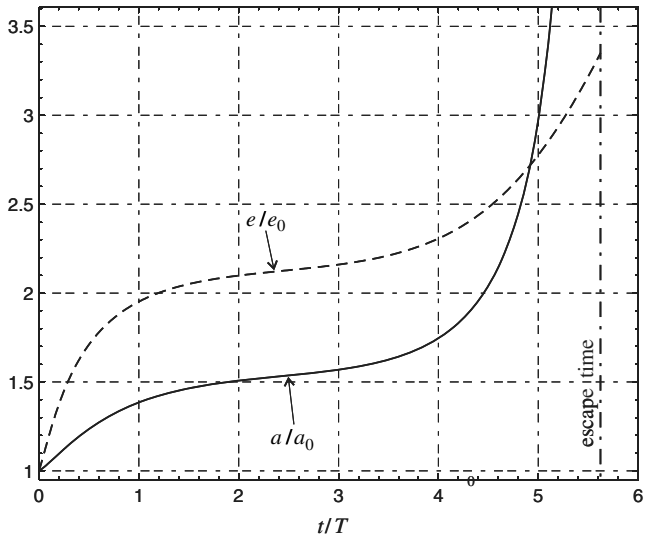

b) Time evolution of orbital parameters

Fig. 3 Spacecraft motion with $e_0 = 0.3$, $\nu_0 = 60$ deg, and $\eta = 1.001\eta^\star$.

where, because the motion is now Keplerian, $\tilde{r}_A$ and $\tilde{r}_P$ coincide with the parking orbit apocenter and pericenter dimensionless distances given by

$$\tilde{r}_A = \frac{a_0(1+e_0)}{r_0}, \qquad \tilde{r}_P = \frac{a_0(1-e_0)}{r_0} \tag{14}$$

In particular, with reference to Fig. 1, $\tilde{r}_A$ coincides with the abscissa of P_0.

Escape Conditions

As stated, an escape condition can be reached by the spacecraft, provided that $\eta > \eta^\star$. The corresponding value of escape distance $\tilde{r}_{\text{esc}}$ is obtained from Eq. (8), setting $\tilde{\mathcal{E}} = 0$. The result is

$$\tilde{r}_{\text{esc}} = 1 - \frac{1}{4\eta\tilde{\mathcal{E}}_0} \tag{15}$$

For example, using the previous data ($e_0 = 0.3$ and $\nu_0 = 60$ deg) and a thrust value $\eta = 0.3$, the escape distance is $\tilde{r}_{\text{esc}} \simeq 3.1$, as shown in Fig. 1. Note that for a circular orbit $\tilde{\mathcal{E}}_0 = -1/2$, and in accordance with [2,3], Eq. (5) reduces to

$$\tilde{r}_{\text{esc}} = 1 + \frac{1}{2\eta} \tag{16}$$

Now consider the problem of calculating $\eta^\star$: that is, the minimum thrust value necessary for attaining an escape condition from a given starting position ν_0. To this end, the polynomial $\mathcal{P}$ in Eq. (12) is rewritten as

$$\mathcal{P} = D(\tilde{r}) + \eta N(\tilde{r}) \tag{17}$$

where

$$N(\tilde{r}) \triangleq 4\tilde{\mathcal{E}}_0^2\tilde{r}^2(\tilde{r}-1) \tag{18}$$

$$D(\tilde{r}) \triangleq \tilde{\mathcal{E}}_0\tilde{r}^2 + \tilde{r} - \mathcal{B} \tag{19}$$

Equation (17) can be translated into a classical Evans' root locus, in which η is treated as a nonnegative parameter. The result is shown in Fig. 4, in which the three branches of the locus correspond to the solutions of $D(\tilde{r}) + \eta N(\tilde{r}) = 0$. Because the roots of $N(\tilde{r})$ are 0 (double) and 1, the root locus shows that α cannot exceed 1. Note that there exists a critical value of thrust ($\eta = \eta^\star$) such that the polynomial $\mathcal{P}$ has a double real root: that is, $\beta(\eta^\star) \equiv \gamma(\eta^\star) \triangleq \beta^\star$. For such a value, one obtains

$$\mathcal{P} = 4\tilde{\mathcal{E}}_0^2\eta^\star(\tilde{r}-\alpha^\star)(\tilde{r}-\beta^\star)^2 \tag{20}$$

where $\alpha^\star \triangleq \alpha(\eta^\star)$.

The breakaway point in Fig. 4 can be obtained using the condition [6]

$$N(\tilde{r})\frac{dD(\tilde{r})}{d\tilde{r}} = D(\tilde{r})\frac{dN(\tilde{r})}{d\tilde{r}} \tag{21}$$

which guarantees the existence of multiple roots for the characteristic equation $\mathcal{P} = 0$. Substituting Eqs. (18) and (19) into Eq. (21), yields

$$\tilde{\mathcal{E}}_0\tilde{r}^3 + 2\tilde{r}^2 - (3\mathcal{B}+1)\tilde{r} + 2\mathcal{B} = 0 \tag{22}$$

where the unique real root corresponds to $\beta^\star$. The critical dimensionless thrust value is obtained by [6]

$$\eta^\star = -\frac{D(\beta^\star)}{N(\beta^\star)} \tag{23}$$

In summary, assuming a critical value of thrust ($\eta = \eta^\star$) and for a given value of initial orbital eccentricity e_0 and spacecraft position ν_0, the polynomial $\mathcal{P}$ can be factorized according to Eq. (20). The isocontour solutions for $\eta^\star$, $\alpha^\star$, and $\beta^\star$ are shown in Figs. 5–7, respectively. For a given pair (ν_0, e_0), $\alpha^\star$ and $\beta^\star$ are the minimum and maximum distances from the primary attainable by a spacecraft in a closed orbit. However, because the roots of $\mathcal{P}$ are found without any explicit constraint on their minimum value, in a realistic mission scenario, it is necessary to check that the resulting value of $\alpha^\star$ be greater than the radius of the primary body.

For a given orbit eccentricity, Fig. 5 shows that the minimum value of $\eta^\star$ (that is, $\eta^\star_{\min} \triangleq \min \eta^\star$) is always attained when the spacecraft is

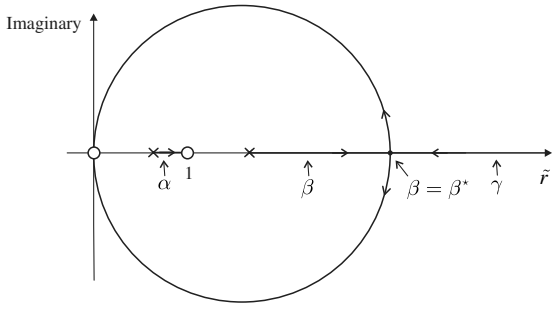

Fig. 4 Roots locus of polynomial $\mathcal{P}$ as a function of $\eta \geq 0$.

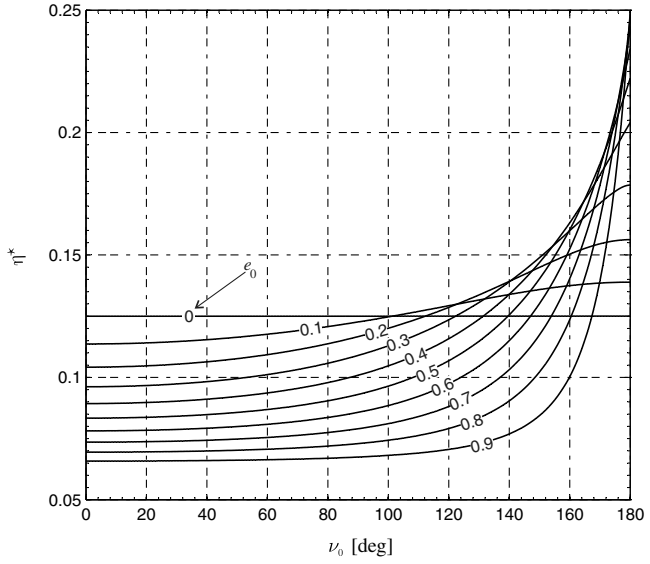

Fig. 5 Minimum dimensionless propulsive acceleration $\eta^\star$ as a function of e_0 and ν_0.

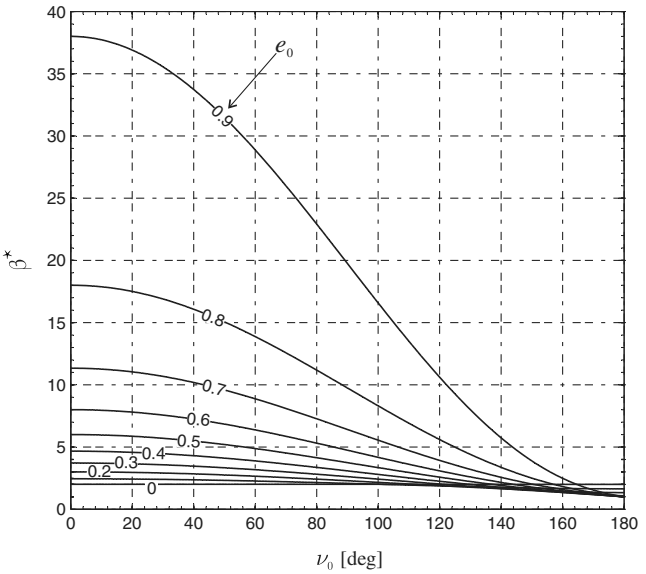

Fig. 7 Maximum apocenter dimensionless distance $\beta^\star$ as a function of e_0 and ν_0.

at the pericenter ($\nu_0 = 0$). The maximum value of $\eta^\star$, instead, is in correspondence of the apocenter. In other terms, the best starting position necessary to minimize the required escape thrust is obtained when the spacecraft is at the parking orbit pericenter.

It is noteworthy that the minimum value of $\eta^\star_{\min}$ has a compact expression. In fact, observing from Eqs. (7) and (10) that $\nu_0 = 0$ corresponds to $\tilde{\mathcal{E}}_0 = (e_0 - 1)/2 = \mathcal{B} - 1$, the polynomial $\mathcal{P}$ of Eq. (12) reduces to

$$\mathcal{P} = 4\tilde{\mathcal{E}}_0^2\eta(\tilde{r} - 1)\left(\tilde{r}^2 + \frac{1}{4\tilde{\mathcal{E}}_0\eta}\tilde{r} + \frac{\tilde{\mathcal{E}}_0 + 1}{4\tilde{\mathcal{E}}_0^2\eta}\right) \tag{24}$$

When η attains its critical value (that is, $\eta = \eta^\star_{\min}$), the polynomial $\mathcal{P}$ can be factorized according to Eq. (20) as

$$\mathcal{P} = 4\tilde{\mathcal{E}}_0^2\eta^\star_{\min}(\tilde{r} - 1)(\tilde{r} - \beta^\star_{\max})^2 \tag{25}$$

where $\beta^\star_{\max} \equiv \beta^\star(\eta^\star_{\min}) = \max \beta^\star$. The condition implied by Eq. (25), that the second-order polynomial between round braces in Eq. (24) has two coincident roots, yields

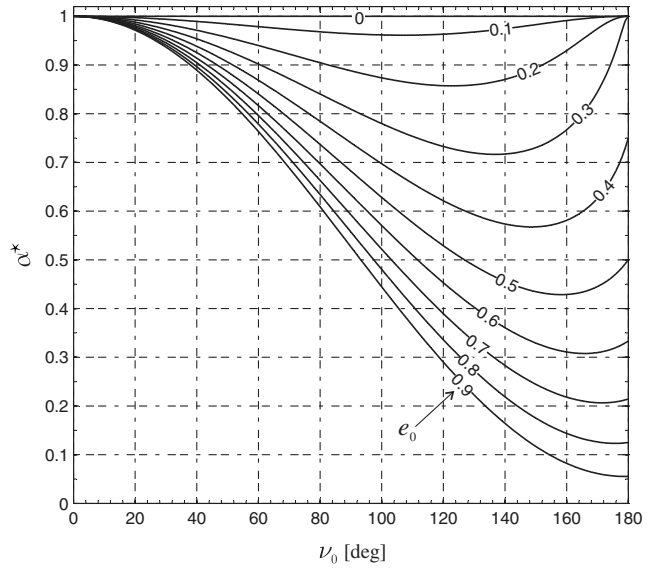

Fig. 6 Pericenter dimensionless distance $\alpha^\star$ as a function of e_0 and ν_0.

$$\eta^\star_{\min} = \frac{1}{8(1 + e_0)} \tag{26}$$

and

$$\beta^\star_{\max} = \frac{2(1 + e_0)}{1 - e_0} \tag{27}$$

The results of Eq. (27) coincide with the values shown in Fig. 7 when $\nu_0 = 0$. Also note from Eq. (25) that $\alpha^\star(\nu_0 = 0) \equiv 1$, in accordance with the results of Fig. 6.

In summary, when an escape mission with a minimum constant radial thrust is involved, the transfer should start at the pericenter of the parking orbit using a propelling acceleration $f_r > f_{r_{\min}}$ with

$$f_{r_{\min}} \triangleq \eta^\star_{\min}\frac{\mu}{a_0^2} = \frac{\mu}{8a_0^2(1 + e_0)} \equiv \frac{\mu(1 - e_0)}{8p_0^2} \tag{28}$$

where $p_0 = a_0(1 - e_0^2)$ is the semilatus rectum of the parking orbit. The corresponding value of escape distance from Eqs. (15) and (26) is

$$r_{\text{esc}} = a_0(5 + 3e_0) \tag{29}$$

Alternatively, when the mission consists of reaching the maximum distance from the primary body without attaining an escape condition, the propulsion system must be set on at the pericenter, and the propelling acceleration must be set equal to $f_{r_{\min}}$ of Eq. (28). The maximum attainable distance from the primary body is

$$r_{\max} = \beta^\star_{\max}a_0(1 - e_0) = 2a_0(1 + e_0) \equiv \frac{2p_0}{1 - e_0} \tag{30}$$

Note that, assuming a circular parking orbit ($e_0 = 0$ and hence $a_0 \equiv r_0$), Eq. (28) provides $f_{r_{\min}} = \mu/(8r_0^2)$, Eq. (29) shows that the escape radius is $r_{\text{esc}} = 5r_0$, and Eq. (30) states that $r_{\max} = 2r_0$, in agreement with the results found in [1–3].

Conclusions

The problem of escape from an elliptic orbit using a constant radial thrust has been discussed in graphical form. The best initial spacecraft position, corresponding to the minimum value of required thrust, coincides with the pericenter of the parking orbit. Assuming such a starting point, an analytical expression for the occurrence of an escape condition has been found. Also, a compact closed-form formula for the maximum amplitude of the radial oscillation if escape

does not occur has been derived. The classical solutions available for circular orbits are recovered by simply setting the eccentricity equal to zero. Therefore, the new results may be thought of as the natural extension to an elliptic orbit of the circular problem.

References

[1] Tsien, H. S., "Take-Off from Satellite Orbit," *Journal of the American Rocket Society*, Vol. 23, No. 4, 1953, pp. 233–236.

[2] Battin, R. H., *An Introduction to the Mathematics and Methods of Astrodynamics*, AIAA Education Series, AIAA, New York, 1987, pp. 408–415.

[3] Prussing, J. E., and Coverstone, V. L., "Constant Radial Thrust Acceleration Redux," *Journal of Guidance, Control, and Dynamics*, Vol. 21, No. 3, May–June 1998, pp. 516–518. doi:10.2514/2.7609

[4] Winglee, R. M., Slough, J., Ziemba, T., and Goodson, A., "Mini-Magnetospheric Plasma Propulsion: Tapping the Energy of the Solar Wind for Spacecraft Propulsion," *Journal of Geophysical Research*, Vol. 105, No. A9, 2000, pp. 21,067–21,078. doi:10.1029/1999JA000334

[5] McInnes, C. R., "Orbits in a Generalized Two-Body Problem," *Journal of Guidance, Control, and Dynamics*, Vol. 26, No. 5, Sept.–Oct. 2003, pp. 743–749. doi:10.2514/2.5129

[6] Franklin, G. F., Powell, J. D., and Emami-Naeini, A., *Feedback Control of Dynamic Systems*, 4th ed., Prentice–Hall, Upper Saddle River, NJ, 2002, pp. 285–286.